

# COMPONENT PART NOTICE

THIS PAPER IS A COMPONENT PART OF THE FOLLOWING COMPILATION REPORT:

TITLE: Minutes of the Explosives Safety Seminar (22nd) Held in Anaheim,  
California on 26-28 August 1986. Volume 2.

TO ORDER THE COMPLETE COMPILATION REPORT, USE AD-A181 275

THE COMPONENT PART IS PROVIDED HERE TO ALLOW USERS ACCESS TO INDIVIDUALLY AUTHORED SECTIONS OF PROCEEDING, ANNALS, SYMPOSIA, ETC. HOWEVER, THE COMPONENT SHOULD BE CONSIDERED WITHIN THE CONTEXT OF THE OVERALL COMPILATION REPORT AND NOT AS A STAND-ALONE TECHNICAL REPORT.

THE FOLLOWING COMPONENT PART NUMBERS COMPRISE THE COMPILATION REPORT:

AD#: P005 350 thru P005 393 AD#: \_\_\_\_\_  
AD#: \_\_\_\_\_ AD#: \_\_\_\_\_  
AD#: \_\_\_\_\_ AD#: \_\_\_\_\_

Accession For	
NTIS GRA&I	<input checked="checked" type="checkbox"/>
DTIC TAB	<input type="checkbox"/>
Unannounced	<input type="checkbox"/>
Justification	
By _____	
Distribution/ _____	
Availability Codes	
Dist	Avail and/or Special
A-1	

AIRBLAST MEASUREMENTS AND EQUIVALENCY  
FOR SPHERICAL CHARGES AT SMALL SCALED DISTANCES

by

Edward D. Esparza  
Southwest Research Institute  
San Antonio, Texas

22nd Department of Defense Explosives Safety Seminar  
26-28 August 1986

AD-P005 385

ABSTRACT

An experimental investigation was conducted to obtain direct measurements of side-on overpressures from spherical charges of six different high explosives at small scaled distances ranging from 0.74 to 3.5 ft/lb<sup>1/3</sup>. The pressure-time recordings of the incident airblast waves were processed to obtain peak side-on overpressures, shock wave arrival times, side-on impulses, and positive durations. Comparisons of the test data were made with standard blast curves for these four parameters. The side-on overpressure and arrival time data from the TNT tests are in excellent agreement with the standard curves. The impulse and duration data show that at scaled distances less than 3 ft/lb<sup>1/3</sup>, the standard curves are not as well defined as those for pressure and arrival time. TNT equivalencies for each of the six explosives were determined using the standard pressure and impulse curves, as well as the actual TNT test data obtained. These results indicate that the pressure based TNT equivalency at small scaled distances for some of the explosives tested can be significantly different than that based on the heat of detonation.

## INTRODUCTION

### Background

Characterization of blast waves from high explosive detonations in free air by experimental methods has a long history dating back to World War II, as reported by Kennedy [1]. Stoner and Bleakney [2] in 1948 reported results of free-air experiments conducted with small TNT and Pentolite charges of various shapes. After World War II, a large number of investigators made free-field blast measurements in the United States. Goodman [3] compiled free-field blast measurements from bare, spherical Pentolite charges made by several investigators at the U.S. Army Ballistic Research Laboratories from 1945 to 1960. During this same time period, data were also generated by investigators at the U.S. Naval Ordnance Laboratory. Baker [4] provides an excellent historical summary and presents much of the data from these investigations.

Measurements of blast parameters from other than free air, high explosive detonations have been made by many investigators, also dating back to World War II. For example, measurements of blast wave properties from ground bursts of large hemispherical TNT charges were compiled and analyzed by Kingery [5]. Air blast data from height-of-burst experiments have been measured by several investigators such as Reisler, et al. [6,7]. Measurements of normally reflected waves have been made by Jack [8], Dewey, et al. [9], Wenzel and Esparza [10], and others. Measurements of blast parameters from charges of various geometries, from sequential detonations, from simultaneous detonations, and at real and simulated altitude conditions have also been made by many investigators [10-17]. Good descriptions of the characteristics of air blast waves in general are provided by Baker [4], Swisdak [18], and Glasstone and Dolan [19].

Because air blast data have been obtained by a large number of investigators for different explosives, one can obtain different predictions for blast parameters depending on the source. In attempts to eliminate some of these variations, "standard" blast parameter graphs and tables have evolved over time. Examples of blast curves are presented in References 4, 5, and 18-21. Probably the most widely used set of standard curves is found in the tri-service manual, "Structures to Resist the Effects of Accidental Explosions" [22]. In this manual, curves for free-air detonations and surface

detonations are presented for various blast parameters. These curves are based partly on experiments, and partly on analyses and computer code computations. At distances very close to the charge, direct measurements of many of the blast parameters are either nonexistent or very few. Consequently, these curves are not well defined at distances close to an explosive charge.

The standard curves are usually for spherical TNT explosions. For other high explosives, the concept of TNT equivalency is then often used to predict the blast parameters. TNT equivalency is defined as the ratio of the charge weight of TNT to the weight of the test explosive that will yield the same amplitude of a blast parameter at the same radial distance from each charge. All high explosives generate blast waves which are quite similar in character. However, their equivalence to TNT may vary with distance from the charge, and with the particular blast parameter chosen for comparison. Thus, a single equivalent weight ratio may not be appropriate, particularly at close distances to the charge where experimental verification may not exist. Furthermore, equivalence based on one blast parameter may be significantly different for another, even though the same high explosive is being tested.

### Objectives

To obtain direct measurements of blast overpressures at small scaled distances from spherical charges of TNT and five other high explosives, Southwest Research Institute (SwRI) funded a project [23] to conduct a series of free-air experiments using explosive charges that were surplus to some earlier SwRI projects. These precision charges ranged in weight from about 0.5 to 1.3 lb and were cast or pressed from Composition B, PBX-9404, Pentolite, TNT, PBX-9501, and PBX-9502. The data from these spherical charges were to be used to characterize the blast waves generated by the six high explosives at small scaled distances. In addition, the TNT data were to be compared to standard curves, and the data from the other five explosives were to be used to analyze the concept of TNT equivalency at small distances from the charges. This paper presents a brief description of the limited number of experiments conducted and the results obtained. Additional details of the tests, and graphs and tabulations of all the experimental data are provided in Reference 23.

## **Blast Scaling**

Scaling of blast wave properties is a common practice used to generalize blast data from high explosives. Scaling or model laws are used to predict the properties of blast waves from large-scale explosions based on tests at a much smaller scale. The most common scaling law is the one formulated independently by Hopkinson [24] and Cranz [25]. This law states that self-similar blast waves are produced at the same scaled distance when two explosives of similar geometry and of the same explosive material, but of different size, are detonated in the same atmosphere. The Hopkinson-Cranz or cube-root scaling law has become so universally used that high explosive blast data are almost always presented in terms of the scaled parameters generated by this law. A more complete discussion of this law is given by Baker [4]. Another widely used scaling law formulated by Sachs [26] allows prediction of the effects of detonations at different ambient conditions. For the experiments reported here, the ambient conditions were not sufficiently different from standard sea level conditions to warrant the use of Sachs' law. Therefore, all data are presented using Hopkinson-Cranz scaled parameters.

## **DESCRIPTION OF EXPERIMENTS**

The experiments were conducted at the SwRI explosives range using the apparatus depicted in Figure 1. Two pipe stands supported wedge-shaped transducer holders, one reconditioned from earlier work [27] and a similar new one. A cross-member was used to suspend the explosive spheres. The transducer wedges were positioned about 5 ft above the concrete pad surface to preclude any surface reflections from interfering with the initial blast wave. In all tests, the wedge-tipped transducer holders were positioned 180° apart on either side of the high explosive spheres. They were 32 in. long, 6 in. wide, and 2 in. thick, were fabricated from 2024-T4 aluminum rectangular stock, and fitted with hardened 4130 steel tips at the wedge-shaped end. Each transducer holder had provisions for mounting six pressure transducers, all in line with the center line of the flat top surface.

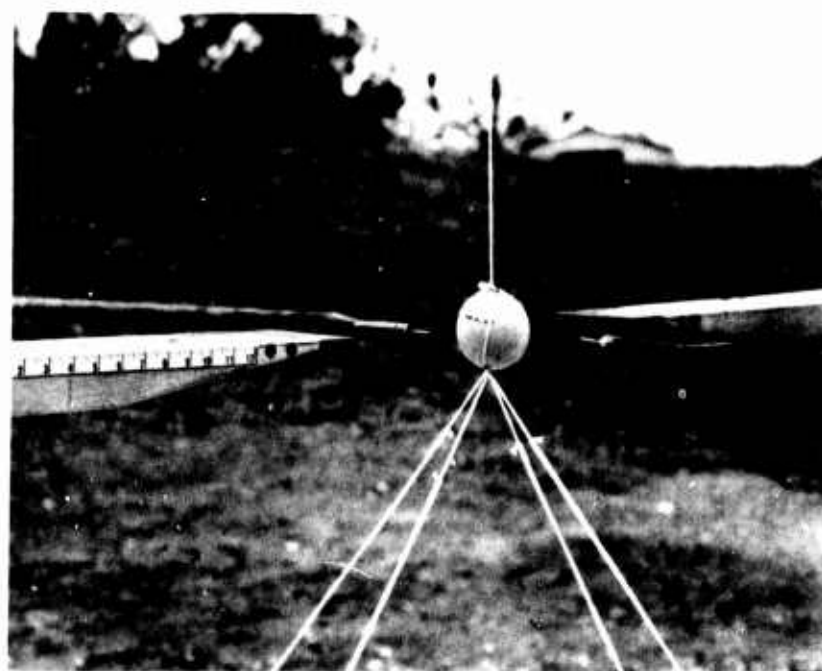
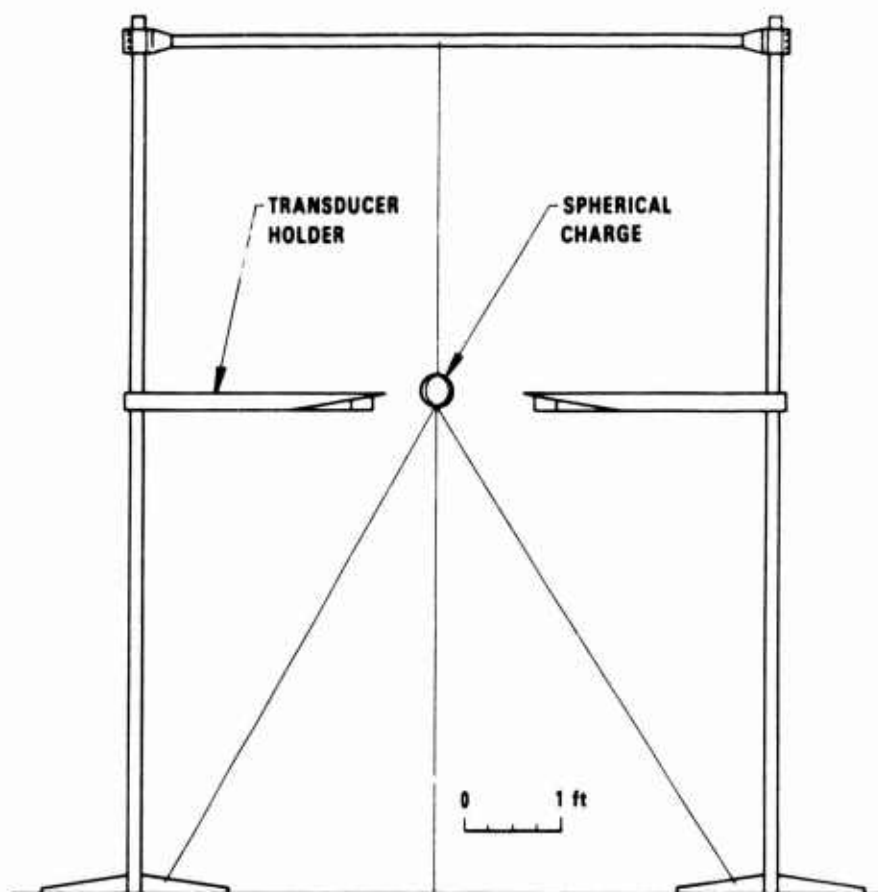


Figure 1. Test Apparatus For Close-in Measurements

The pressure transducers used to measure the blast overpressures are manufactured by PCB Piezotronics. Three different models of the series 102A transducers were used. All models have the same physical configuration differing primarily in their full scale range, sensitivity, and discharge time constant. Each PCB transducer utilizes a piezoelectric, pressure sensing element made of quartz which is coupled with a miniature source follower within the body of the transducer. Power and signal amplification were provided with PCB Model 494A06 six channel units. The blast pressure-time histories were recorded on magnetic tape using a Honeywell Model 101, Wideband II, FM tape recorder at a bandwidth of 0-500 kHz (+1, - 3dB).

The data were processed in sets of four data channels using a Biomation Model 105 transient recorder for digitizing at effective sampling rates of 0.6 to 3.2 million samples per second depending on the measurement location. The digital data were transferred from the transient recorder memory via a CAMAC data buss to a hard disk and a flexible diskette of a DEC 11/23 computer located at the range facility. Final data processing and plotting were then accomplished from the diskette with a DEC 11/70 computer. Figure 2 shows a block diagram of the pressure data record/reduction system. The high-frequency response of this system was 200 kHz.

In addition to the pressure measurements, pin gages of the piezoelectric and ionization types were used to obtain additional time-of-arrival data. Both types used are made by Dynasen, Inc. They were epoxied into copper tube mounts which were held in place by special adapters and pipe stands. The pin gages using the stands were positioned horizontally looking at the center of the sphere and at 90° from the pressure transducer holders. When installed on a test, pin gage tips were located 2 in. and 4 in. from the charge surface. In some cases a third pin was used with the tip on the surface of the charge. This pin was suspended almost vertically along the string holding the charge in place.

## EXPERIMENTAL RESULTS AND DISCUSSION

Test data were obtained from 18 experiments using six different types of high explosives as indicated in Table 1. For some of the explosives, more than one explosive weight was available for testing. The pressure-time

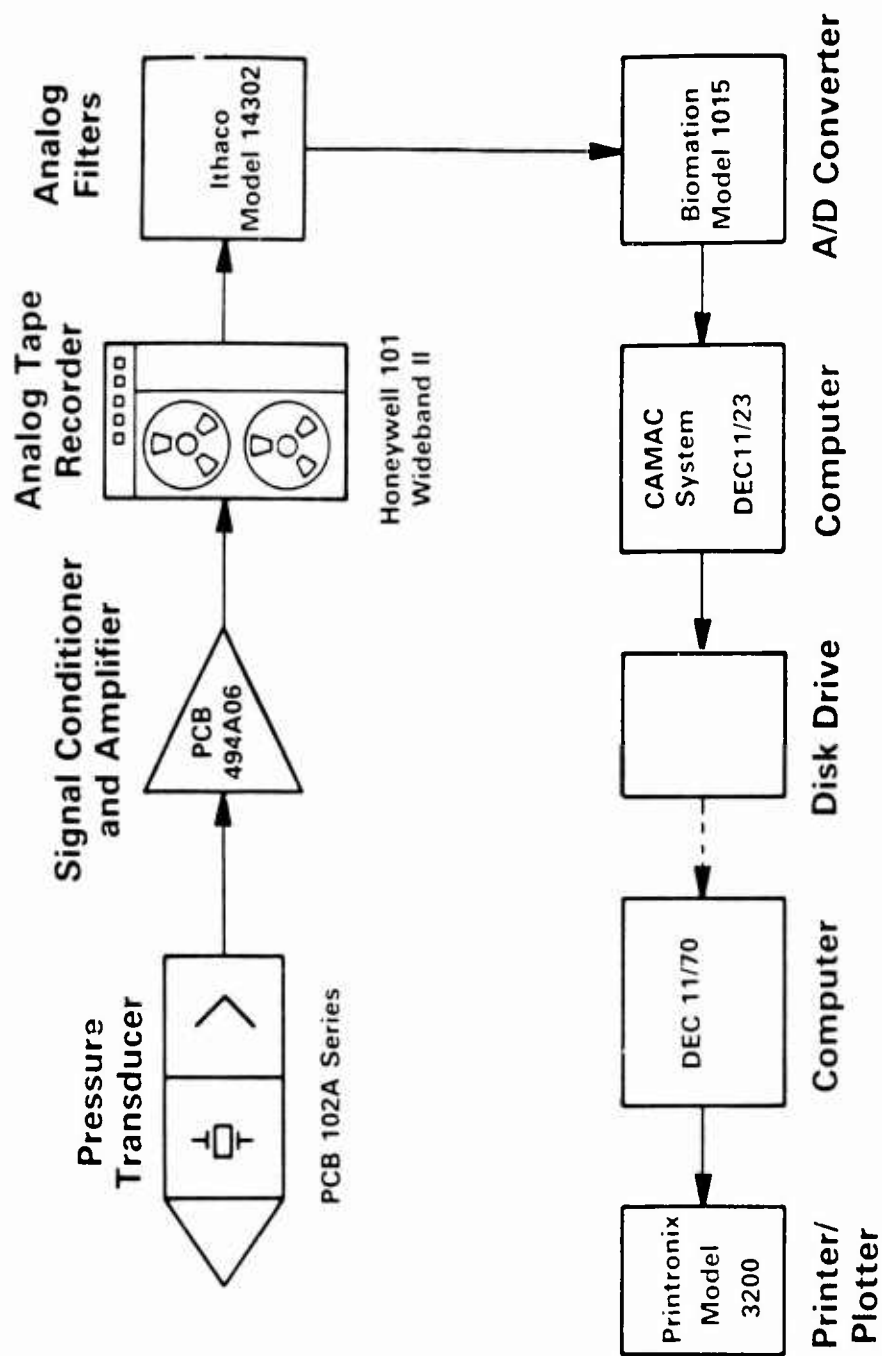


Figure 2. Data Recording and Processing System



recordings made on each test were processed to obtain peak side-on (incident) overpressures, shock wave arrival times, side-on impulses, and positive durations of the incident pressure pulse. Additional arrival time data were obtained with the position pins. The pressure data were obtained at scaled distances ranging from 0.74 to 3.5 ft/lb<sup>1/3</sup>. In most tests, 12 pressure measurements were made. Arrival time data were obtained at scaled distances as close as the surface of the explosive sphere on some tests.

More than 200 pressure measurements were made in this research program. The shock wave in air from any high explosive is formed when the detonation wave propagating in the explosive reaches the surface. For a spherical charge initiated at the center, the initial shock wave in air will also be spherical, and, consequently, symmetrical about any plane bisecting the charge. High explosives generate blast waves which are quite similar in character. However, the properties of the waves may differ for different explosives, particularly at close proximity. The wave formed in air adjacent to an explosion has properties much influenced by the nature of the explosive source. Once the wave propagates in air independently of its source, it is affected primarily by the properties of air. As the blast wave passes through the air, rapid variations of blast wave properties (such as pressure) occur. The properties which are usually defined and measured are those of the undisturbed or side-on wave as it propagates through the air. Examples of side-on overpressures recorded on this project are shown in Figures 3-6.

Table 1. Summary of Experiments

<u>Explosive Type</u>	<u>Nominal Charge Weight (lb)</u>	<u>No. of Experiments</u>
Composition B	1.074	2
Composition B	0.494	1
PBX-9404	0.495	4
PBX-9404	1.002	3
Pentolite	1.309	3
TNT	1.285	2
PBX-9501	0.805	2
PBX-9502	1.301	1

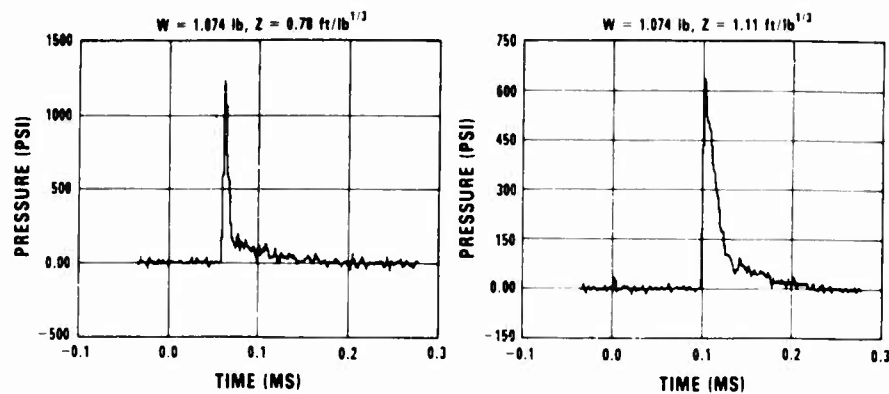


Figure 3. Blast Pressure Data From a Composition B Test

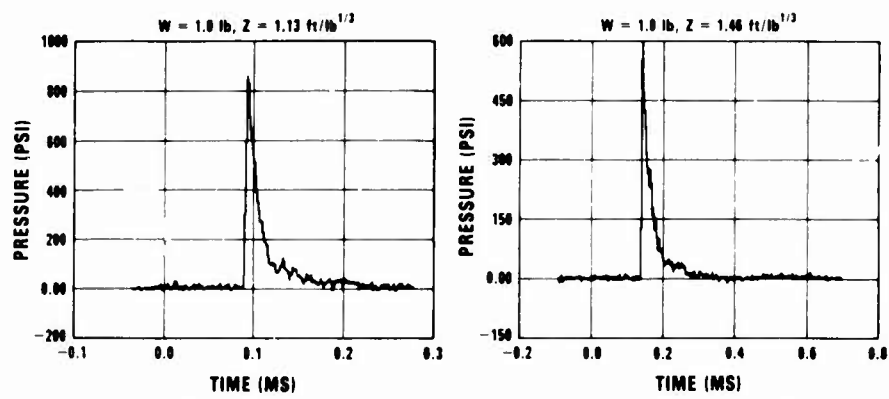


Figure 4. Blast Pressure Data From a PBX-9404 Test

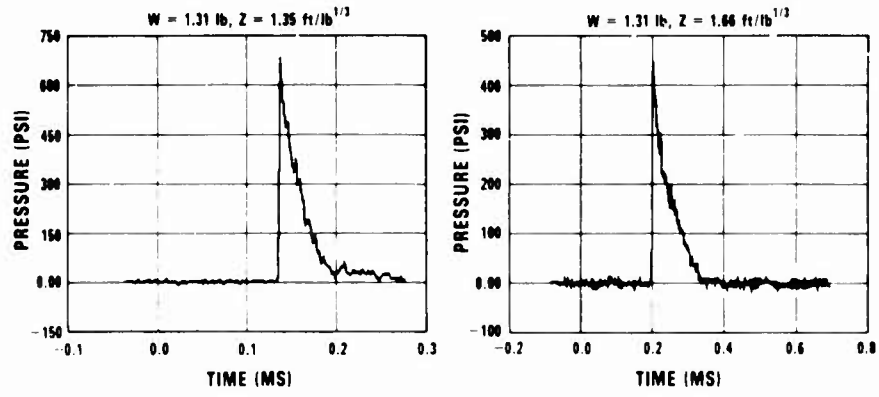


Figure 5. Blast Pressure Data From a Pentolite Test

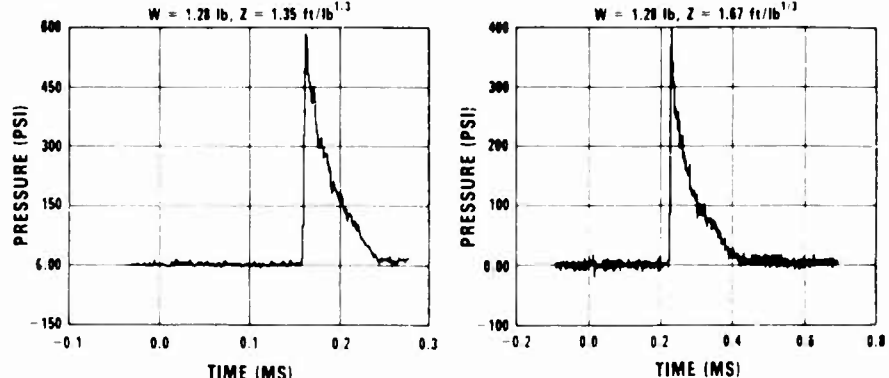


Figure 6. Blast Pressure Data From TNT Tests

Figure 3 presents pressure-time histories recorded at scaled distances ( $Z$ ) of 0.78 and 1.11 ft/lb<sup>1/3</sup> on a test using a sphere of Composition B with a mass ( $W$ ) of 1.074 lb. In Figure 4, two measurements from a PBX-9404 test are presented. The first of these two pressure measurements was taken at a scaled distance of 1.13, about the same as for the second trace in Figure 3. These two traces exemplify the similarity in the character of the data obtained at the same scaled distance from two different explosives. However, the magnitudes of the pressures measured are different. Figure 5 includes a sequence of two measurements made on a Pentolite test at scaled distances  $Z$  of 1.35 and 1.66. As was the case with the previous two figures, these two traces depict the gradual decay in the peak pressure with increasing distance, as well as the gradual increase in arrival and duration times. Figure 6 shows two data traces from TNT tests at scaled distances of 1.36 and 1.67, similar to those for the Pentolite data of Figure 5. These last two figures again show the similarity in the character of the incident overpressures from two different high explosives at similar scaled distances and the differences in amplitude.

The pressure measurements made on this program covered a range in scaled distances from 0.74 to 3.5 ft/lb<sup>1/3</sup>. The examples of data presented concentrated on the closer scaled distances. However, examination of the data plots showed consistency at all scaled distances within each test and within tests using the same type of high explosive, even for those cases in which more than one charge size was available for testing. The observed rise times for the closer-in pressure measurements were approximately 3 microseconds. This value is consistent with the measurement system upper frequency response specification. At the larger scaled distances, the rise times observed were about 7 microseconds, which agree with the time required for the blast wave to travel across the pressure transducer diaphragm.

#### TNT Data Comparisons

Peak incident or side-on overpressure ( $P_s$ ) was the primary blast parameter measured on this project. The peak overpressure at the shock front of an air blast wave can be measured directly with pressure transducers or it can be inferred from the velocity of the shock front. All measurements reported here were made directly with pressure transducers located at small scaled distances from the spherical high explosive charges. The arrival time ( $t_a$ ) of a free-air blast wave is defined here as the time interval between the

initiation of the detonator and the arrival of the blast wave at a measurement location. This interval of time includes the time for the detonation wave to travel through the charge. Measurement of arrival times can be accomplished by several techniques. It can be done using high speed cinematography, blast switches of various types, or pressure transducers. Arrival time is usually the most accurately measured blast parameter. In this program, most measurements were obtained from the pressure transducer records. Some additional data at closer scaled distances were obtained with pin gages. The specific side-on impulse ( $i_s$ ) is the positive area under the pressure-time history. The side-on impulse is a function of the peak overpressure, the duration of the positive phase, and the rate of decay of the pressure behind the shock front. Of the four blast parameters measured on this project, the positive duration ( $t_d$ ) is the most subjective measurement. Individual interpretations of the same data will vary and inherently will produce a larger scatter than on the other three blast parameters.

Pressure-time records were obtained from two TNT experiments with spheres weighing 1.285 lb. The four parameters measured on these tests are plotted in Figures 7-10 and are compared to TNT standard curves [28] which will be included in the revised edition of the tri-service manual, Reference 22. The peak overpressures measured are plotted in Figure 7. The new test data [23] are plotted as vertical bars indicating the range measured. These data were measured at scaled distances ranging from 0.75 to 2.59 ft/lb<sup>1/3</sup>. The new TNT pressure data are self-consistent and the comparison with the reference curve and most of the data base used to develop this curve indicates good agreement. This confirms the validity of the data from the TNT experiments as well as the data from the tests using the other five high explosives since the same measurement system and test procedures were used. Also, it increases the confidence of the results presented later on TNT-equivalency based on peak incident pressures.

It is interesting to note that the TNT reference curve for pressure from Reference 28 is a polynomial curve fit to pressure values found primarily in References 3, 5-7, 18, and 29. The compiled data from Goodman [3] are for Pentolite spheres. These data were converted in Reference 28 to TNT equivalents for use in the TNT curve fit. The TNT equivalency used is not given. For scaled distances less than 1.5 ft/lb<sup>1/3</sup>, all the peak pressures presented

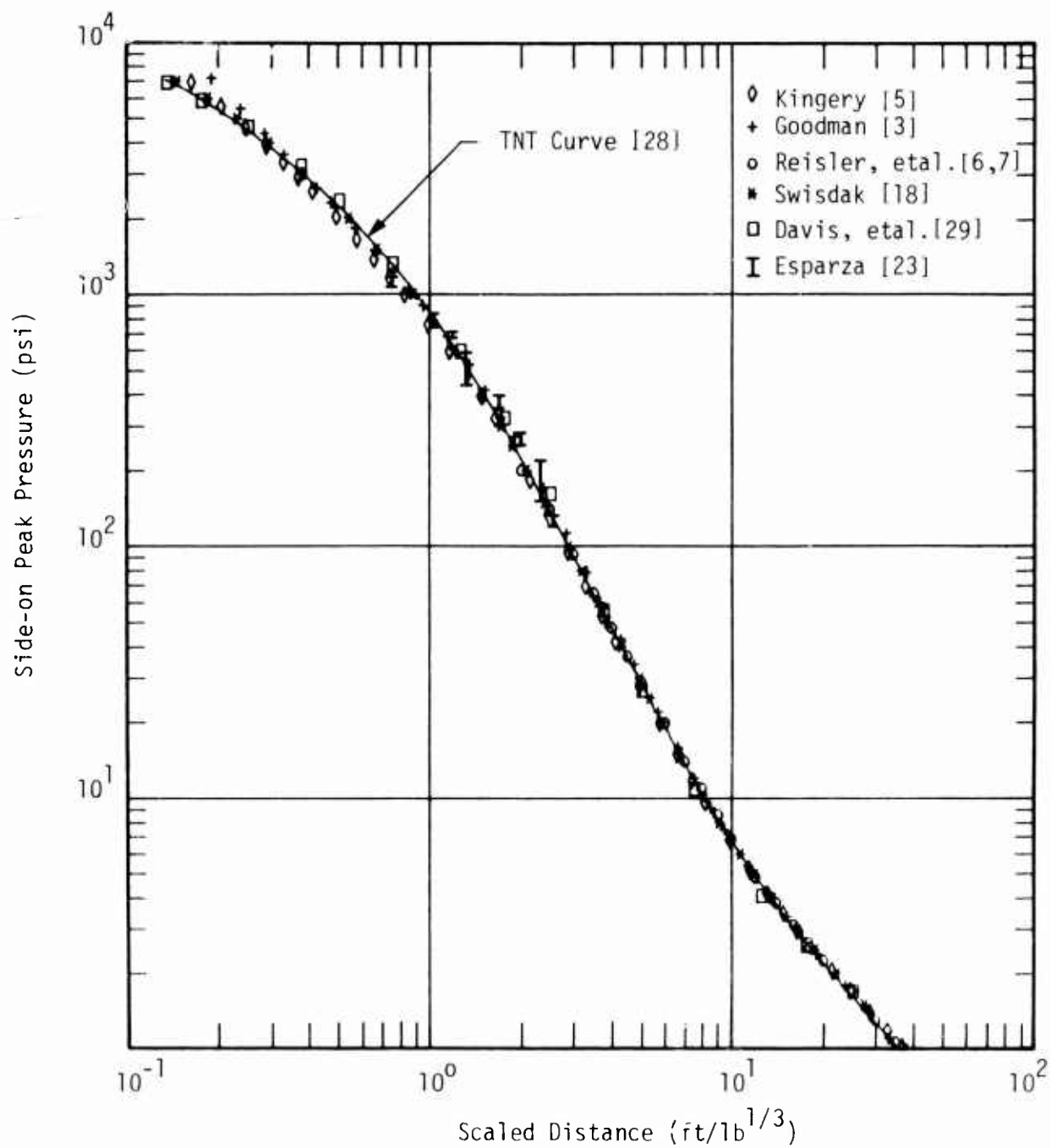


Figure 7. Comparison of TNT Pressure Data With TNT Curve

by Goodman [3] were obtained by Sultanoff and McVey [30] from optical measurements of shock front velocities. The data reported by Kingery [5] are from TNT surface bursts and are converted in Reference 28 to free air equivalent data using a reflection factor of 1.8. The pressure measurements from Reisler, et al. [6,7], were from TNT tests, but are all for scaled distances greater than  $2.0 \text{ ft/lb}^{1/3}$ . Swisdak [18] states that, at scaled distances less than  $1.0 \text{ ft/lb}^{1/3}$ , all overpressures given in that reference were obtained by hydrodynamic computer code calculations. Reference 29 presents TNT data tables and curves which were taken from Dobbs, et al. [31], and are identical to those in Reference 22, the tri-service manual. None of these last three references [22, 29 and 31] indicates which portions of the curves are derived from actual measurements. Thus, the lack of actual TNT incident pressure measurements at small scaled distances indicates that even the revised TNT standard curve from Reference 28 is not well defined experimentally close to the charge, and that the new pressure measurements presented in this paper are an important contribution to the experimental data base.

In Figure 8, the scaled time-of-arrival data for the TNT experiments are plotted as vertical bars showing the range of measurements at each scaled distance. As expected, the scatter of the data is less than for the corresponding incident pressure data, and the scatter increases the closer the measurements were made to the charge center. The TNT test data show excellent agreement with the TNT curve from Reference 28. The arrival time of the shock wave at a distance from an explosion depends on the velocity of the wave. The Rankine-Hugoniot equations relate the velocity of a shock front and the peak pressure of the shocked gas. Thus, it is possible to compute the velocity of the shock front from known values of peak incident overpressure and in turn compute arrival times from the derived shock velocities. This is the approach taken in Reference 28 to develop the scaled arrival time curve so that it was consistent with calculated shock velocities and the side-on pressure curve shown in Figure 7. Thus, the new measured arrival times are also consistent with the side-on pressure measurements.

The incident impulse data from the TNT tests [23] are presented in Figure 9. Over the range of scaled distance shown, the measured scaled impulses define a curve which indicates an explosive less energetic than TNT. This result is unlike the peak pressure and arrival time data which agreed with the

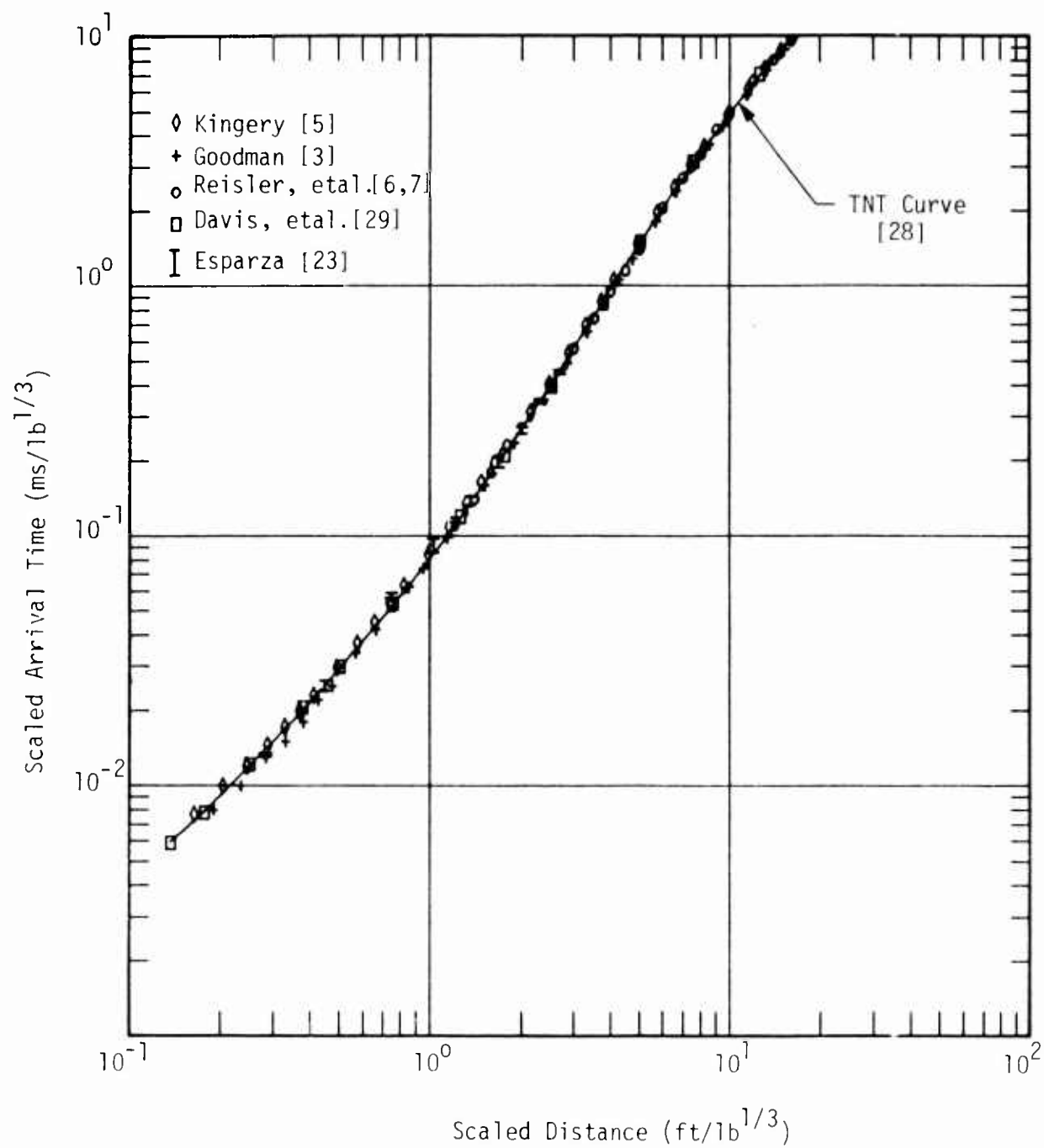


Figure 8. Comparison of TNT Arrival Time Data With TNT Curve

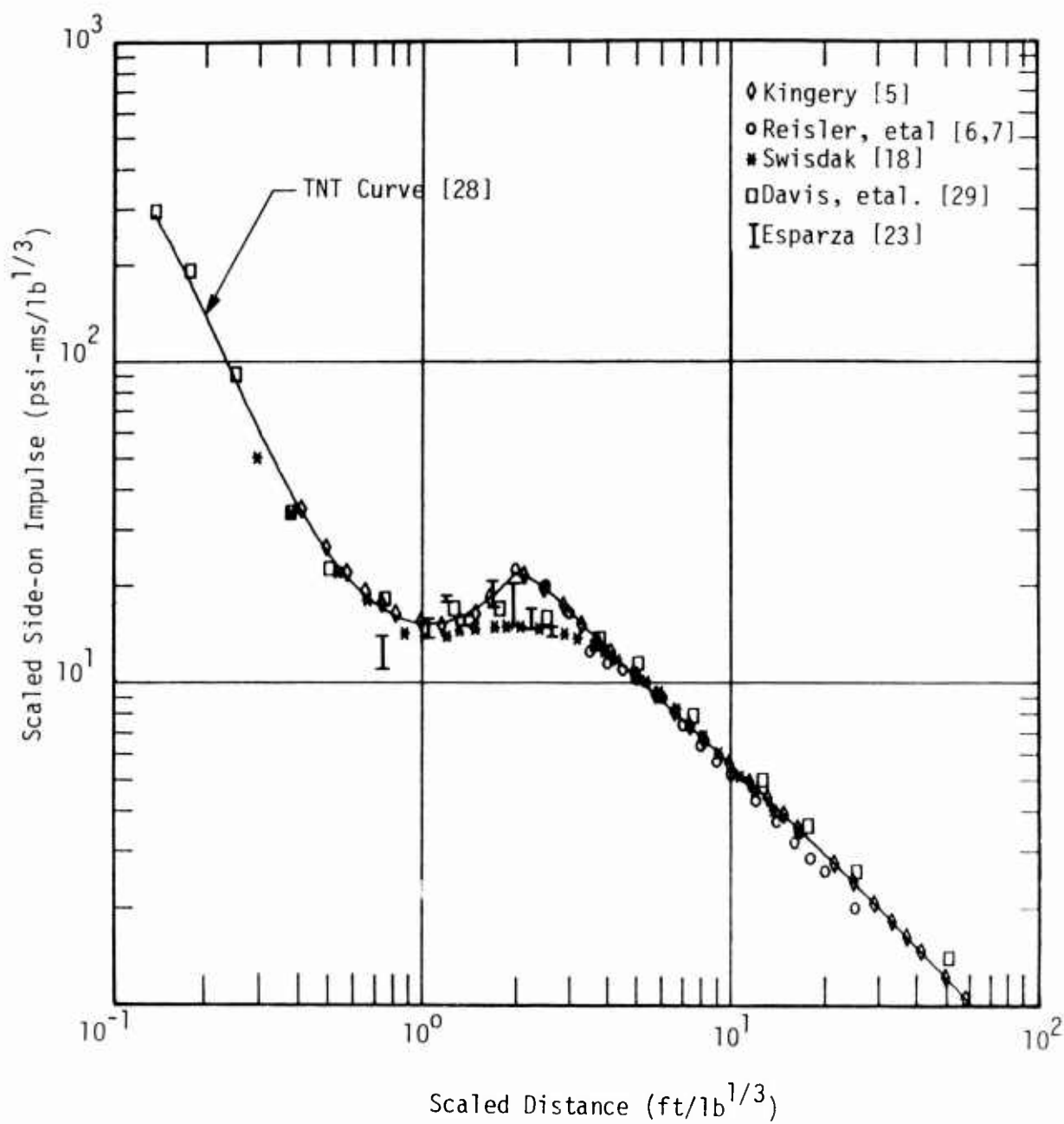


Figure 9. Comparison of TNT Impulse Data With TNT Curve

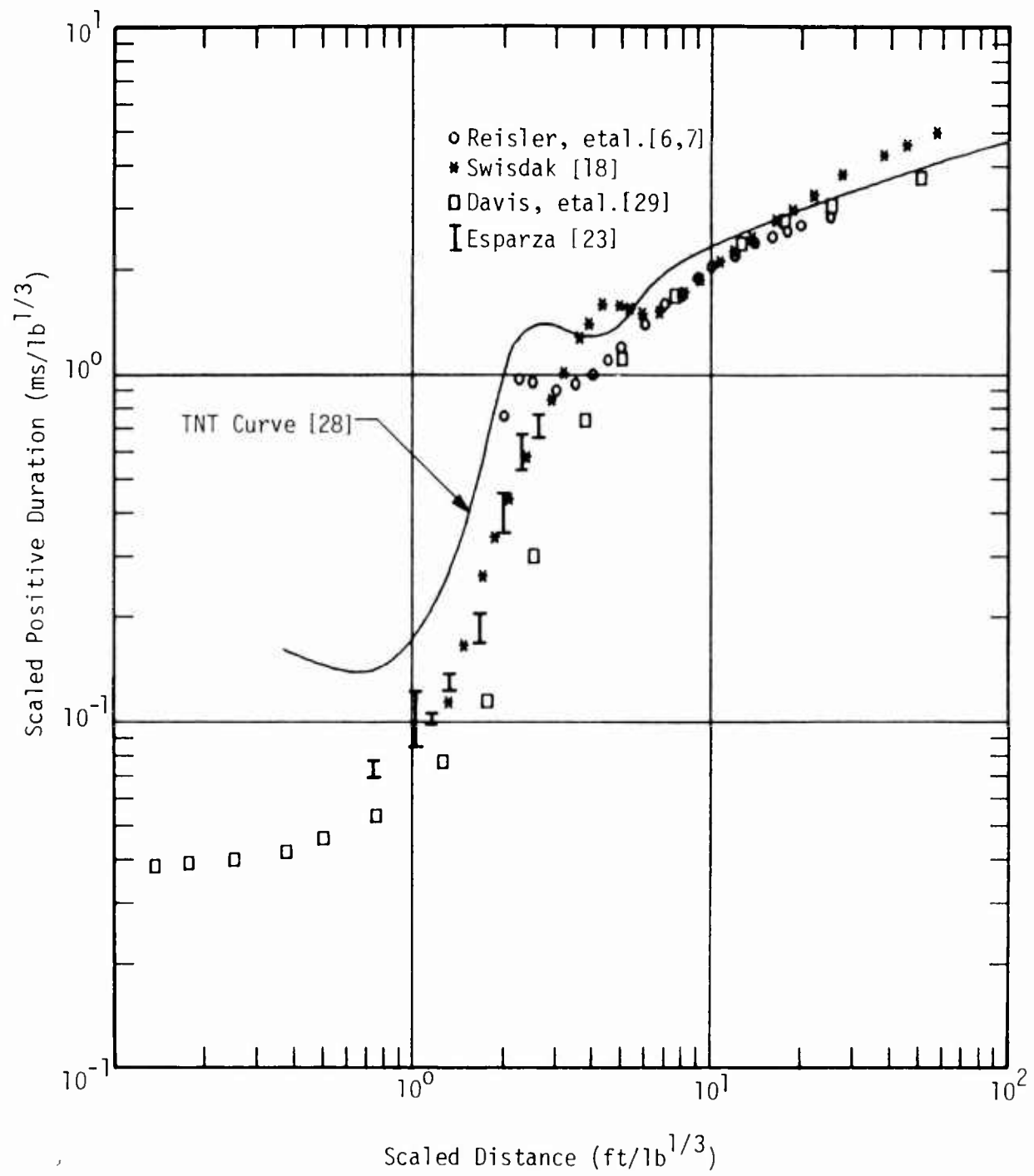


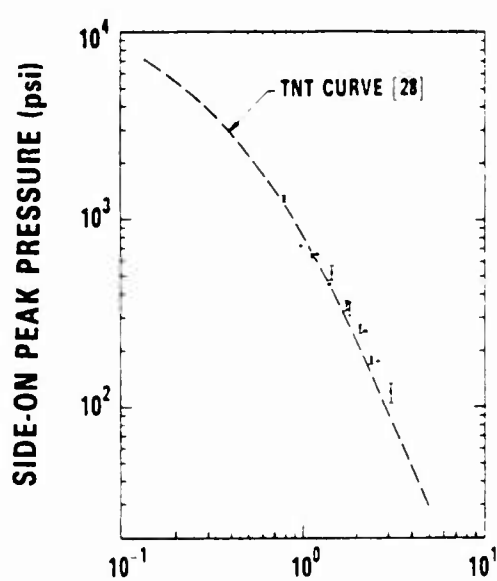
respective reference curve. However, the range of scaled distances at which the new impulse data [23] were obtained is the same at which major differences are indicated in the data from the referenced literature presented in Figure 9 used to define the TNT curve from Reference 28. In fact, more weight appears to have been given to data converted to free air equivalents from surface and height-of-burst explosions in defining the side-on impulse TNT curve [28], than actual free air data like those measured on this project. Furthermore, the new TNT test data were measured over a scaled distance range of 0.75 to 2.59 ft/lb<sup>1/3</sup> which includes that portion of the curve with changes in slope, making it the most difficult portion of the curve to define with experiments or curve fits.

Figure 10 is a plot of the new TNT duration data [23] compared to the TNT reference curve and data from other references included in Reference 28. This comparison shows consistently shorter scaled durations for the new test data than the reference curve at respective scaled distances. Over the range of scaled distances at which measurements were made, the scaled times from the reference curve are almost a factor of two longer than the new measured values. The curve fit for the reference TNT curve was based only on data from hemispherical TNT surface bursts assuming a 1.8 reflection factor to convert them to free-air equivalents [28]. However, the other free air, TNT data shown in Figure 10 from References 18 and 29 show the same type of differences between the curve and the new data. The TNT reference curve appears to be more of an upper bound on the scale duration data at scaled distances less than 3 ft/lb<sup>1/3</sup>.

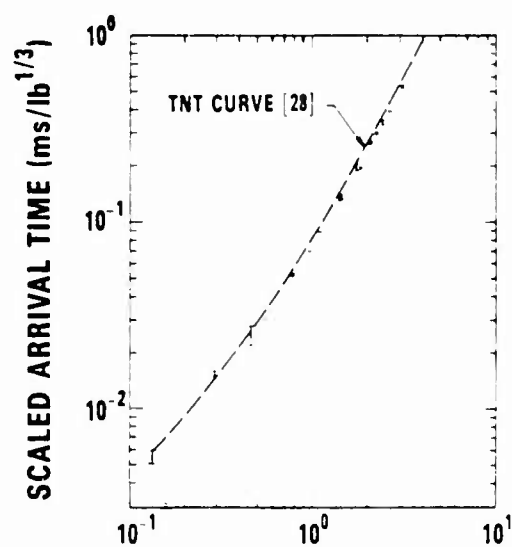
#### Data From Other Explosives

Measurements of  $P_s$ ,  $t_a$ ,  $i_s$ , and  $t_d$  for the five other explosives listed on Table 1 were also made. For some of them, two charge weights were available for testing; for some, there was only one charge size. As shown in Figures 3-6, the pressure-time records at comparable scaled distances are quite similar in character, but the various parameters may differ quantitatively. For example, the measured data obtained from the three Composition B experiments are presented in Figure 11. Two tests used 1.07-lb spheres and one test used a 0.494-lb sphere. In Figure 11a, the peak pressure data obtained over a scaled distance range of 0.78 to 3.1 ft/lb<sup>1/3</sup> are self-consistent and in general were of higher amplitude than the comparable TNT



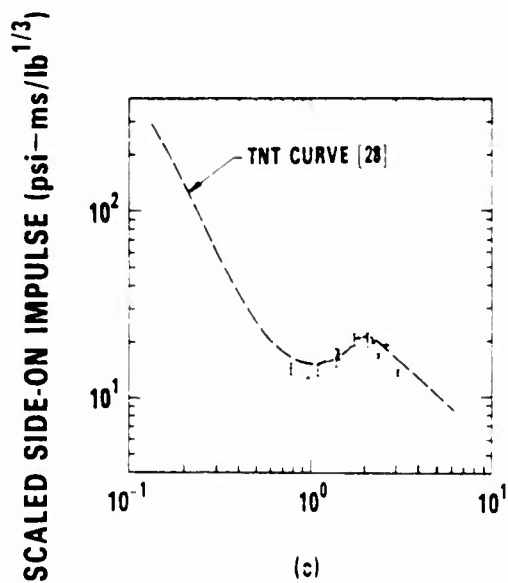


(a)

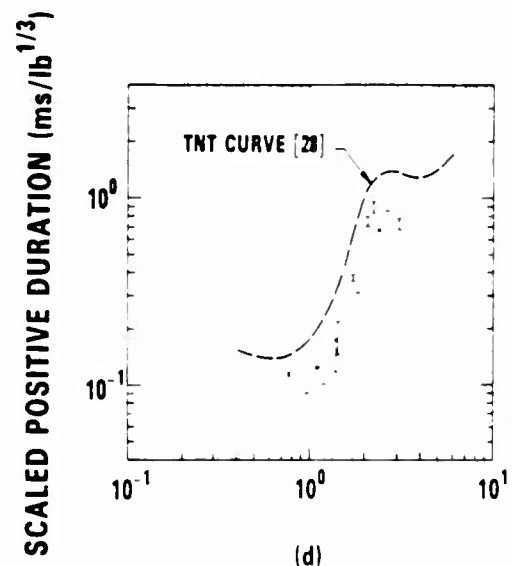


(b)

SCALED DISTANCE ( $\text{ft}/\text{lb}^{1/3}$ )



(c)



(d)

SCALED DISTANCE ( $\text{ft}/\text{lb}^{1/3}$ )

Figure 11. Blast Data from Composition B Experiments

values denoted by the dashed curve taken from Reference 28. This indicates that based on peak pressure measurements, Composition B is more energetic than TNT. Additional discussions on TNT equivalency are presented later in the paper. The Composition B arrival time data are graphed in Figure 11b. Most of the arrival times measured for this explosive are slightly shorter than those indicated by the TNT reference curve [28]. In Figure 11c, the impulse data from the Composition B tests are presented. Generally, the data are of somewhat lower amplitude than indicated by the TNT reference curve [28]. Note that, on a plot of scaled impulse versus scaled distance, an explosive less energetic than TNT, with a constant equivalency, would yield a parallel curve shifted left and down at  $45^\circ$  from the TNT curve. Figure 11d presents the scaled durations from the Composition B tests. It is obvious from this figure that the scatter in the duration data is greater than for other three blast parameters as was the case with the TNT data presented previously.

In Reference 23, similar data comparisons with the TNT reference curves from Reference 28 are also made for the other four high explosives tested. In this paper those results will be summarized. The peak overpressures generated by PBX-9404, Pentolite, and PBX-9501 were of higher amplitude than those indicated for the TNT reference curve. Only the pressures from PBX-9502 were of lower amplitude than the TNT values. The arrival time measurements for these four explosives exhibited less scatter than the pressure data, but were consistent with them. Thus, of the six high explosives tested only the scaled arrival times from the PBX-9502 tests were slower than the TNT values. This result is consistent with that obtained from the overpressure data.

The impulse data from the PBX-9404 tests were generally of higher amplitude than those from the TNT reference curve, while those for the Pentolite tests were generally of lower amplitude. The impulse data from the PBX-9501 tests were in some cases slightly lower and in other cases higher than the TNT reference curve. Finally, the impulse data from the one PBX-9502 test were generally of lower amplitude than analogous TNT curve values. Thus, of the six high explosives tested, only two generated impulse data that were consistently of the same or higher amplitude than the reference TNT curve [28] at scaled distances ranging from 0.74 to  $3.5 \text{ lb/ft}^{1/3}$ .

As already shown for the TNT and Composition B tests, the positive duration data from the other four explosives tested had greater scatter than any of the other three blast parameters measured. In addition, the scaled durations were in every case significantly shorter than those from the TNT reference curve [28].

### Pressure TNT Equivalency

It is common practice to express the blast effects from various explosive sources in terms of the amount of TNT that will produce a blast wave having the same property as the one being characterized. Side-on pressure is the most common parameter used to determine TNT equivalency for high explosives. TNT equivalency based on incident pressure is defined as the ratio of the charge weights (TNT weight/explosive weight) that will give the same peak pressure at the same radial distance from each charge.

The concept of TNT equivalency offers the advantage of providing in one number an identification of a given blast wave in terms of a standard explosive whose blast effects have been extensively documented. The disadvantages are in many instances minor, but must be considered whenever TNT equivalency is applied, particularly at small scaled distances. In the first place, most explosives have not been tested sufficiently or at all at small scaled distances to determine a good equivalency factor based on pressure or other blast parameters. Second, the equivalency factor may vary with scaled distance or may differ whether based on pressure or another parameter. Finally, for high explosives with no comparative data available, TNT equivalency is often approximated by the ratio of the two heats of detonation. This ratio may be adequate at some scaled distances and invalid at others.

Computations of TNT equivalent factors were made for the six explosives tested in this project using the incident pressure data obtained on the 18 experiments. For each explosive, plots of pressure versus scaled distances were made and an approximate fit was made through the average of the pressures measured at each scaled distance. TNT equivalency ratios were computed by determining the scaled distances corresponding to pressures of 100, 320, and 1,000 psig. For TNT, these three incident pressures corresponded to scaled distances of 2.89, 1.69, and  $0.9 \text{ ft/lb}^{1/3}$  as obtained from the reference TNT curve [28]. The pressure equivalency  $E_p$  for an explosive is then

$$E_p = \frac{W_{TNT}}{W} = \left( \frac{Z}{Z_{TNT}} \right)^3 \quad P_s = \text{constant} \quad (1)$$

where:

- $E_p$  = TNT equivalency of an explosive based on side-on overpressure
- $P_s$  = peak side-on overpressure
- $R$  = distance from the center of the charge
- $W$  = explosive mass
- $W_{TNT}$  = TNT mass
- $Z$  = scaled distance =  $R/W^{1/3}$
- $Z_{TNT}$  = scaled distance =  $R/W_{TNT}^{1/3}$

The average equivalency for each explosive was obtained by calculating  $E_p$  at each of the three pressures and then averaging the three values. The equivalency ratio for each explosive varied slightly over the pressure range of 100 to 1000 psig and the average value and corresponding standard deviation are tabulated in Table 2.

The values listed in Table 2 are based on a limited number of experiments. However, the peak pressures measured were self-consistent for each explosive and the range of the data at each measurement location was for the most part within  $\pm 10\%$  of the average. In addition, the TNT experiments generated peak pressures which agreed very closely with values from the TNT

Table 2. Average Pressure TNT Equivalency

<u>Explosive Type</u>	<u>Pressure TNT Equivalency *</u>	<u>Standard Deviation</u>
Composition B	1.2	11%
PBX-9404	1.7	18%
Pentolite	1.5	5%
TNT	1.0	7%
PBX-9501	1.6	5%
PBX-9502	0.9	2%

\*For incident pressure range of 100-1000 psig

curve from Reference 28. This reference curve is the result of a polynomial curve fit to large amounts of data from tests and some from computer calculations compiled from 10 different references.

Comparisons of the TNT equivalency ratios based on the pressure data obtained on this project and those based on heats of detonations and other references are presented in Table 3. It is interesting that for some explosives the equivalency ratio based on the pressure data at small scaled distances agrees quite well with that based on the heats of detonation. For other explosives significant differences are apparent. Also, the ratios from Reference 18 are based on a much lower pressure range except for Pentolite whose equivalency ratio agrees well with the new value. The pressure range for the ratios from Reference 22 is given as being applicable from 2 to 50 psi. Note that, since TNT equivalency is the ratio of the weights of TNT to that of a test explosive, the effect on the scaled distance is the cube root of the ratio. In other words, for a particular explosive that is supposed to be 50% more energetic than TNT (TNT equivalency of 1.5) the effect on the scaled distance ( $R/W^{1/3}$ ) becomes only 14.5%. The expected average peak pressure for this more energetic explosive would be about 28% higher than for a comparable weight of TNT at a scaled distance of 1.0 ft/lb<sup>1/3</sup>. At other small

Table 3. Comparisons of TNT Equivalency Ratios

Explosive Type	Pressure TNT Equivalency	Based on Calculated Heat of Detonation*	From Ref. 18	From Ref. 22
Composition B	1.2 (100-1000 psi)	1.09	1.11 (5-50 psi)	1.10 (2-50 psi)
PBX-9404	1.7 (100-1000 psi)	1.11	1.13 (5-30 psi)	---
Pentolite	1.5 (100-1000 psi)	1.09	1.40 (5-600 psi)	1.17 (2-50 psi)
TNT	1.0 (100-1000 psi)	1.00	1.00 (Standard)	1.00 (2-50 psi)
PBX-9501	1.6 (100-1000 psi)	1.13	---	---
PBX-9502	0.9 (100-1000 psi)	0.82	---	---

\* From References 21, 32, and 33

scaled distances the effect on the average peak pressure would be different, but generally the effect is less on the pressure than on explosive weight.

Conversely, note that in determining TNT equivalency ratios a small variation in determining the scaled distances for a particular average peak pressure is amplified because the ratio of scaled distances is cubed as indicated in Equation 1. Thus, it would be difficult to compute a TNT equivalency ratio at a given scaled distance more accurate than about  $\pm 10\%$ . To obtain an accuracy of  $\pm 10\%$  requires that the scaled distance for a particular average peak pressure generated by an explosive be determined more accurately than  $\pm 3\%$ .

### Impulse TNT Equivalency

The second parameter that is sometimes used to compute TNT equivalency is the side-on impulse. Computations were made of TNT equivalent ratios based on the impulse data obtained for the six explosives tested at small scaled distances. A similar procedure was used as for the pressure data. The impulse equivalency  $E_i$  for an explosive is simply

$$E_i = \frac{W_{TNT}}{W} = \left( \frac{Z}{Z_{TNT}} \right)^3 \quad i_s = \text{constant} \quad (2)$$

where:

$E_i$  = TNT equivalency of an explosive based on side-on impulse  
 $i_s$  = side-on impulse

However, on a plot of scaled impulse ( $i_s/W^{1/3}$ ) versus scaled distance ( $R/W^{1/3}$ ), constant values for  $i_s$  are found at lines oriented  $45^\circ$  to the scaled axes. Thus, the graphical or computational procedure is somewhat more involved than for pressure. Since the test data were measured at small scaled distances over which the TNT reference curve has two different inflection points, computations were made at scaled distances of 0.9 and 2.9 ft/lb<sup>1/3</sup> and averaged to obtain equivalency ratios based on impulse. The results are presented in Table 4.



Table 4. Average Impulse TNT Equivalency Base on Impulse

<u>Explosive Type</u>	<u>Impulse TNT Equivalency Using TNT Ref. Curve [28]</u>	<u>Impulse TNT Equivalency Normalized to TNT Data</u>
Composition B	0.8 (11%)	1.3
PBX-9404	1.2 (47%)	2.0
Pentolite	0.6 ( 8%)	1.0
TNT	0.6 (14%)	1.0
PBX-9501	1.0 ( 6%)	1.7
PBX-9502	0.7 ( 6%)	1.1

Unlike the excellent agreement between the pressure data from the TNT tests and the TNT reference curve, the TNT impulse data indicated an equivalency significantly less than unity when compared to the TNT impulse curve from Reference 28. This difference is probably due to "the very few and sometimes suspect quality" [28] of the measured incident impulses at scaled distances less than  $1 \text{ ft/lb}^{1/3}$ , and the wide scatter of the data used to generate the reference curve between a scaled distance of 1 and  $3 \text{ ft/lb}^{1/3}$  [28], the range over which most of the measurements reported here were made. In fact, as shown in Figure 9 the reference curve appears to be an upper bound of the scaled impulse over this range of scaled distances. It is not surprising, then, that the test data from the present TNT tests yielded an equivalency ratio less than 1 when compared to the curve from Reference 28. Consequently, the TNT equivalency ratios obtained using the reference curve and the data from the six high explosive tests were normalized to the values of the new TNT data. These results are also tabulated in Table 4 and show a more realistic relationship among the impulse equivalencies, as well as a reasonable comparison with the corresponding pressure equivalences presented in Table 2. However, as has been shown by others [18,29], the ratios for pressure and impulse are not necessarily the same.

#### SUMMARY

An experimental program was conducted to obtain direct measurement of side-on overpressure at small scaled distances from spherical charges of six different high explosives. The pressure-time recordings made on the 18

experiments were processed to obtain peak overpressures, shock wave arrival times, side-on impulses, and positive durations of the incident or side-on pressure pulse. In addition to comparisons of the data with TNT reference curves for these four parameters, TNT equivalency for each explosive was obtained based on the measurements of side-on peak overpressures and impulses. More than 200 pressure measurements were made on tests with six different high explosives: TNT, Composition B, PBX-9404, Pentolite, PBX-9501, and PBX-9502. The number of tests conducted was limited by the number of spherical charges left over from previous projects.

The observations and conclusions based on the peak overpressure data were:

- o data were self-consistent for each explosive
- o in most cases variations from the average pressure at each scaled distance were less than  $\pm 10\%$
- o compared to a TNT reference curve [28], the TNT data showed excellent agreement
- o only PBX-9502 was less energetic than TNT based on the overpressure data.

From the arrival times measured the following can be stated about these data:

- o arrival time data exhibited less scatter than the pressure data
- o TNT test data agreed quite closely with a TNT reference curve [28]
- o comparisons for all six explosives with a TNT reference curve [28] showed consistency with similar comparisons based on pressure.

Comparisons of the impulse data to the TNT reference curve [28] showed that

- o in general, the test data were of lower amplitude for four of the explosives, and of the same or higher amplitude for the other two explosives
- o by using the TNT test data as the basis for comparison, more realistic impulse-based equivalencies were obtained.

Comparisons were also made for the positive duration data from each explosive and the reference TNT curve [28]. This showed that:

- o the scaled durations measured for all six explosives were shorter than those indicated by the reference TNT curve

- o over the range of scaled distances used to make the measurements, the reference curve appears to be more of an upper bound for the new data as it is for the data from other sources [28].

Even though only a limited number of spherical charges were available, the experimental data obtained on this project [23] for the six different high explosives are an important addition to the very limited air burst data (and are in some cases the only known data) available from direct pressure measurements for characterizing their blast parameters at small scaled distances. The side-on pressure and arrival time data from the TNT tests are in excellent agreement with the revised curves in Reference 28. Similar data for the other five explosives show differences that indicate TNT equivalency for some of them can be significantly different than that based on their heat of detonation. The impulse and duration data showed that at scaled distances less than  $3 \text{ ft/lb}^{1/3}$ , the revised standard TNT curves [28] are definitely not as well defined as those for pressure and arrival time. More experimental air burst data are needed from TNT tests, as well as from other commonly used high explosives to better define TNT equivalency at small scaled distances based on impulse.

Additional experiments similar to those described in this report are recommended to measure pressure-time histories at small scaled distances from spherical charges. These additional data would better characterize the blast waves near different high explosives and increase the confidence of the new data presented. The experimental techniques used on this project to make the pressure measurements are suitable to obtain data at scaled distances as small as  $0.75 \text{ ft/lb}^{1/3}$ . However, even closer direct measurements of pressure may be possible using small, scaled hemispherical charges detonated on a replaceable hardened steel surface with side-on transducers mounted flush with the steel surface.

#### ACKNOWLEDGEMENTS

This paper is based on a research project funded by Southwest Research Institute (SwRI) through its Advisory Committee for Research. Special thanks are extended to Dr. W. E. Baker for his invaluable advice and technical consultation in the proposing and performance of the project this paper is

based on. The author appreciates the important contributions made by the SwRI project team to the successful conduct of that project and the resources provided by SwRI for the preparation of this paper.

#### REFERENCES

1. Kennedy, W. D., "Explosions and Explosives in Air," in **Effects of Impact and Explosion**, M. T. White (ed.), Summary Technical Report of Div. 2, NDRC, Vol. I, Washington, DC, AD 221 586, 1946.
2. Stoner, R. A., and Bleakney, W., "The Attenuation of Spherical Shock Waves in Air," **Journal of Applied Physics**, Vol. 19, No. 7, 1948.
3. Goodman, H. J., "Compiled Free Air Blast Data on Bare Spherical Pentolite," BRL Report 1092, Aberdeen Proving Ground, MD, February 1960.
4. Baker, W. E., **Explosions in Air**, University of Texas Press, Austin, Texas, 1973.
5. Kingery, C. N., "Air Blast Parameters versus Distance for Hemispherical TNT Surface Bursts," BRL Report No. 1344, Aberdeen Proving Ground, MD, September 1966.
6. Reisler, R., Pellet, B., and Kennedy, L., "Air Blast Data from Height-of-Burst Studies in Canada, Vol. I: HOB 5.4 to 71.9 Feet," BRL Report No. 1950, Aberdeen Proving Ground, MD, December 1976.
7. Reisler, R., Pettit, B., and Kennedy, L., "Air Blast Data from Height-of-Burst Studies in Canada, Vol. II: HOB 45.4 to 144.5 Feet," BRL Report No. 1990, Aberdeen Proving Ground, MD, May 1977.
8. Jack, W. H., Jr., "Measurements of Normally Reflected Shock Waves from Explosive Charges," BRL Memorandum Report No. 1499, Aberdeen Proving Ground, MD., AD 422886, July 1963.
9. Dewey, J. M., Johnson, O. T., and Patterson, J. D., II, "Mechanical Impulse Measurements Close to Explosive Charges," BRL Report No. 1182, Aberdeen Proving Ground, MD, November 1962.
10. Wenzel, A. B., and Esparza, E. D., "Measurements of Pressures and Impulses at Close Distances from Explosive Charges Buried and in Air," Final Report on Contract No. DAAK 02-71-C-0393 with U. S. Army MERDC, Ft. Belvoir, VA, August 1972.
11. Wisotski, J. and Snyder, W. H., "Characteristics of Blast Waves Obtained from Cylindrical High Explosives Sources," DRI No. 2286, Denver, CO, 1965.
12. Reisler, R. E., Giglio-tos, L., and Teel, G. D., "Air Blast Parameters from Pentolite Cylinders Detonated on the Ground," BRL Memorandum Report No. 2471, Aberdeen Proving Ground, MD, 1975.
13. Kulesz, J. J., Esparza, E. D., and Wenzel, A. B., "Blast Measurements at Close Standoff Distances for Various Explosive Geometries," **Minutes of the 18th Explosives Safety Seminar**, Vol. I, San Antonio, TX, Department of Defense Explosives Safety Board, September 1978.

14. Guerke, G. and Scheklinski-Glueck, G., "Blast Parameters from Cylindrical Charges Detonated on the Surface of the Ground," **Minutes of the 20th Explosives Safety Seminar**, Vol. I, Norfolk, VA, 1982; and **Proceedings I, Eighth International Symposium on Military Applications of Blast Simulation**, Spiez, Switzerland, 1983.
15. Zaker, T. A., "Blast Pressures from Sequential Explosions," IIT Research Institute, Chicago, Illinois, Phase Report II, Project J6166, March 25, 1969.
16. Hokanson, J. C., Esparza, E. D., Wenzel, A. B., and Price, P. D., "Measurements of Blast Parameters on a Barricade Due to Simultaneous Detonations of Multiple Charges," Contractor Report ARLCD-CR-78032, U. S. Army Armament Research and Development Command, Dover, NJ, 1978.
17. Jack, W. H., and Armendt, B. F. Jr., "Measurements of Normally Reflected Shock Parameters under Simulated High Altitude Conditions," BRL Report No. 1280, Aberdeen Proving Ground, MD, AD 469014, April 1965.
18. Swisdak, M. M., Jr., "Explosion Effects and Properties: Part I--Explosion Effects in Air," NSWC/WOL/TR 75-116, Naval Surface Weapons Center, White Oak, Silver Spring, MD, October 1975.
19. Glasstone, Samuel and Dolan, Philip J., "The Effects of Nuclear Weapons," United States Department of Defense and U. S. Department of Energy, 1977.
20. "Suppressive Shields Structural Design and Analysis Handbook," U. S. Army Corps of Engineers, Huntsville Division, HNDM-1110-1-2, November 1977.
21. **A Manual for Prediction of Blast and Fragment Loadings on Structures**, U. S. Department of Energy, DOE/TIC-11268, 1980.
22. **Structures to Resist the Effects of Accidental Explosions**, Department of the Army Technical Manual TM-5-1300, Department of the Navy Publication NAVFAC P-397, Department of the Air Force Manual AFM 88-22, Department of the Army, the Navy, and the Air Force, June 1969.
23. Esparza, E. D., "Side-on Blast Measurements and Equivalency at Small Scaled Distances for Spherical Charges," Final Report 06-9386, Southwest Research Institute, San Antonio, Texas, May 1985.
24. Hopkinson, B., British Ordnance Board Minutes 13565, 1915.
25. Craz, C., **Lehrbuch der Ballistic**, Springer-Verlag, Berlin, 1926.
26. Sachs, R. G., "The Dependence of Blast on Ambient Pressure and Temperature," BRL Report 466, Aberdeen Proving Ground, MD, 1944.
27. Esparza, E. D., and Baker, W. E., "Measurements of Blast Waves from Bursting Pressurized Frangible Spheres," NASA CR-2843, Washington, DC, May 1977.
28. Kingery, C. N., and Bulmash, G., "Airblast Parameters from TNT Spherical Air Burst and Hemispherical Surface Burst," Ballistic Research Laboratory Technical Report ARBRL-TR-02555, Aberdeen Proving Ground, MD, April 1984.
29. Davis, V. W., Goodale, T., Kaplan, K., Kriebel, A. R., Mason, H. B., Melichar, J. F., Morris, P. J., and Zaccor, J. N., "Nuclear Weapons Blast Phenomena, Volume IV--Simulation of Nuclear Airblast Phenomena with High Explosives (U)," DASA Report 1200-IV, Washington, DC, July 1973 (SECRET-FRD).

30. Sultanoff, M. and McVey, G., "Shock-Pressure at and Close to the Surface of Spherical Pentolite Charges Inferred from Optical Measurements," BRL Report No. 917, Aberdeen Proving Ground, MD, August 1954.
31. Dobbs, N., Cohen, E., and Weissman, W., "Blast Pressures and Impulse Loads for Use in the Design and Analysis of Explosive Storage and Manufacturing Facilities," **Annals of the New York Academy of Sciences**, Vol. 152, Art 1, October 1968.
32. Hokanson, J. C., Esparza, E. D., Baker, W. E., Sandoval, N. R., and Anderson, C. E., "Determination of Blast Loads in the DWF," Volume 1, Phase II, SwRI-6578, San Antonio, TX, July 1982.
33. Dobratz, B. M. and Crawford, P. C., "Properties of Chemical Explosives and Explosive Simulants," LLNL Explosives Handbook, Lawrence Livermore National Laboratory, January 1985.